Cellulose (2024) 31:7003–7013
https://doi.org/10.1007/s10570-024-06007-3

ORIGINAL RESEARCH

Revealing pore size distribution in cellulose and lignin-cellulose man-made fibers – effect of draw ratio and lignin content

Jenny Bengtsson · Erica Johnsson · Hanna Ulmefors · Tobias Köhnke · Thaddeus Maloney

Received: 23 February 2024 / Accepted: 5 June 2024 / Published online: 14 June 2024

Abstract There are limited methods available for measurement of the porosity of cellulose fibers, even more so for obtaining a pore size distribution. Conventional pore analysis methods require dry samples, with intact pores. However, pores in cellulose fibers collapse when dried from water and thus present a challenge for sample analysis. Furthermore, the pore collapse is partially irreversible which should be accounted for in the analysis. In this study, analysis of pore structure was carried out in the wet state with thermoporometry and also for critical point dried samples, analyzed with N_2 sorption. This study determines the effect of fiber lignin content and certain spinning parameters on the pore size distribution of spun fibers before and after drying. It could also be concluded that solvent exchange, drying from a non-polar solvent will result in an altered pore size distribution, with a total pore volume greater than if dried from water, however not representative of the never-dried state. It is concluded that thermoporometry together with the water retention value (WRV) measurement is a powerful combination to acquire insights to the pore size distribution of spun fiber.

Keywords Cellulose · Lignin · MMCF · Thermoporometry · Porosity

Introduction

There are many reasons for substituting fossil-based fibers with biobased alternatives from natural polymers such as cellulose. For example, they offer the potential of lower climate impact (Shen et al. 2012), and give rise to less persistent micro fibrous pollution (Zhang et al. 2021). Man-made cellulose fibers (MMCF) are produced via solution spinning techniques, such as air-gap spinning. In order to meet the requirement of a certain application, or promote resource efficiency, cellulose may also be blended with other biopolymers. Using powerful solvents like ionic liquids, cellulose has been blended with several other biopolymers such as lignin (Ma et al. 2015; Bengtsson et al. 2018; Protz et al. 2021), chitin (Ota et al. 2021) and keratin (Kammiovirta et al. 2016; Fang et al. 2023). Previous research has demonstrated that cellulose-lignin hybrid fibers are a promising candidate for making biobased carbon fibers (Hermansson et al. 2019; Bengtsson et al. 2022).

Supplementary Information The online version contains supplementary material available at https://doi.org/10.1007/s10570-024-06007-3.

J. Bengtsson (✉) · E. Johnsson · H. Ulmefors · T. Köhnke
Fiber Development, Department of Polymer, Fiber and Composites, RISE Research Institutes of Sweden, Argongatan 30, 431 53 Mölndal, Sweden
e-mail: jenny.bengtsson@ri.se

T. Maloney
Department of Bioproducts and Biosystems, School of Chemical Engineering, Aalto University, 00076 Aalto, Finland

Alterations in the solution spinning process affect the final fiber properties. In air-gap spinning, an extensively studied spinning parameter is the draw ratio, i.e. the difference between the extrusion and take-up velocity and thus a measure of how much the fiber has been stretched during spinning. A higher draw ratio during spinning induces molecular orientation within the cellulose fibers (Michud et al. 2016; Svenningsson et al. 2019), both in the crystalline and amorphous domains (Gubitosi et al. 2021). Consequently, the tensile strength of the fiber increases with draw ratio up to a saturation level (Cui et al. 2022).

The porosity of such fibers, and how it is affected by spinning parameters and mixture of polymers is, however, generally an overlooked feature. The distribution of voids within the fiber will influence, for example, its absorbency and strength. As mentioned above, lignin-cellulose fibers can be used as precursor fibers for biobased carbon fiber. It is known that the strength of carbon fibers is sensitive to pores within the fibers, and it is therefore of great interest to investigate how the addition of lignin to a cellulose fiber affects its' porosity. Pores in MMCFs have been observed in TEM, by staining of the fibers with a contrasting medium (Abu-Rous et al. 2006). Information on average pore size and volume within a cellulose fiber can also be gathered from small angle X-ray measurements (Hribernik et al. 2016), and neutron scattering measurements (Sharma et al. 2019), where a decrease in the average pore size with draw ratio has been reported (Cui et al. 2022).

For determining the pore size distribution (PSD) methods like N_2 sorption can be used, although it requires completely dry fibers. However, it is known that cellulose undergoes 'hornification' during drying: including that pores close irreversibly and do not regenerate upon rewetting. The decreased accessibility of lyocell fibers upon drying has been visualized with reduced dye uptake (Abu-Rous et al. 2007), and lowering of the water retention value (WRV) (Kongdee et al. 2004). Thus, it has been found that in order to achieve reliable measurements of cellulose in BET (Brunauer–Emmett–Teller) measurements, the cellulose needs to be dried in a more open state. Solvent exchange may be used to preserve at least some of the water swollen pores (Hedlund et al. 2019). However, contraction of cellulose pulp fibers has been observed when changing from a water to cyclohexane swelled state, indicating closure of pores (Wang et al. 2003). Consequently, it would be preferable to be able to analyze the microstructure of never-dried fibers.

Analyzing the porosity of cellulose fibers bin the as-spun, never-dried, state is however challenging and there are only a few methods available. The total pore volume of cellulose can be correlated to the water retention value (WRV) which has been extensively used for cellulose pulp fibers (Maloney et al. 2023), and some reports with dried MMCF (Kongdee et al. 2004). Methods that can analyze pore size distribution of cellulose in the wet state, and thus never-dried MMCF, are thermoporometry (Koistinen et al. 2023), cryo NMR (Östlund et al. 2013), and fiber saturation point (Luukko and Maloney 1999). Thermoporometry and cryo NMR utilizes that water inside pores will freeze at a suppressed temperature, which is dependent on the diameter of the pore.

Thermoporometry is based on the melting temperature depression of water held in cell wall pores and application of the well-known Gibbs-Tomson equation to determine PSD. It is suitable for the measurement of mesopores (less than 50 nm pore diameter). Water retention value (WRV) is a centrifuge technique than can be used to measure the total fiber pore volume, also including macropores (greater than 50 nm). Thus, WRV complements well thermoporometry and is included in this study. PSD from N_2 sorption of critical point dried samples is also most applicable in the mesopore range. This technique is compared to thermoporometry.

The overall aim of this work is to evaluate the impact of draw ratio during spinning, and the addition of lignin to a cellulose fiber, on the pore structure of both never dried and dried fibers.

Experimental

Materials

Dissolving pulp with the addition of lignin was used in the production of regenerated fibers. Softwood kraft lignin was produced at the LignoBoost Demo (Bäckhammar, Sweden) with the LignoBoost process. The Klason lignin content of the lignin was 94%, and detailed information on the lignin characteristics is available in Bengtsson et al. 2018. Softwood Kraft dissolving-grade pulp produced by Georgia Pacific (Atlanta, GS, USA) with an intrinsic viscosity of 465 ml/g determined according to ISO 5351:2010

was used. Lyocell fibers were purchased from Lenzing AG (Austria). The ionic liquid 1-ethyl-3-methyl imidazolium acetate (EMIMAc, 95%) was purchased from Sigma-Aldich (Steinhemin, Germany).

Fiber spinning

The pulp was ground to improve the solvent impregnation. Cellulose and lignin were dissolved in EMIMAc in a closed reactor, heated to 70 °C and stirred at 30 rpm for one hour using an anchor impeller. After blending, the mixture was transferred to the container used during spinning and deaeration was performed at 60 °C below 10 kPa pressure for at least 12 h to remove excess air from the dope.

Spinning of the fibers was performed with a piston pump bench setup system. The dope was extruded through a 33-hole spinneret with a capillary diameter of 100 µm and a length to diameter ratio (L/D) of 2, with an extrusion speed of 4 m/min. The container for the solution had a temperature of 45 °C or 60 °C dependent on solution used. The air gap was 1 cm and the coagulation solvent used was deionized water with at a temperature of 2 – 5 °C. A cellulose sample was collected by extruding cellulose solution and coagulated without applying any tension and referred to as coagulated cellulose. The fibers were collected at draw ratio 1 or 2, and the rolls with fibers were stored in deionized water below 10 °C. Never-dried and dried fibers were collected and compared. Fibers were dried with constant length at 60 °C for 30 min, to a dry content of 95%.

Delignification and solvent exchange

Lignin was leached from cellulose-lignin filaments by a 70:30 acetone:water solution. Never dried filaments were submerged in the solution for a total time of 2 days and the solution was replaced 5 times, until no coloration of the liquid occurred. Approximate concentration of filaments in the liquid was 1 wt%. (0.1 g filament in 10 ml). The used lignin is soluble up to at least 10 wt% in the acetone–water mixture, that is no saturation occurred. Pure cellulose fibers where exposed to the same procedure for a comparative sample. The leached filaments were dried from a non-polar solvent to prevent collapse of the structure during drying. The solvent exchange was done by first replacing the acetone–water mixture with dry acetone and later cyclohexane. (Köhnke et al. 2011; Larsson et al. 2013) For each solvent the filaments were left in liquid for 2 days and the liquid was replaced ten times.

Mechanical properties of fibers

Mechanical properties of fibers were determined using a Vibroskop (Lenzing Instruments, Lenzing, Austria) that induces vibration and then adjusts the length of the fiber to obtain resonance. The titer was then used to measure the tenacity and elastic modulus (cN/tex) with a Vibrodyn (Lenzing Instruments). This instrument performs a tensile stretch of the fiber until breakage. All measurements were performed in a controlled climate with a temperature of 20 ± 2 °C and relative humidity of $65 \pm 4\%$.

Fiber porosity

For the WRV measurement 100–200 mg dried fibers were used. All fibers were cut into 1 cm pieces and soaked in deionized water for 1 h before placing them in the centrifuge filter tube 50 ml, 30×115 mm style. The filter used was Whatman GF/C glass microfiber filters 1.2 µm and the used instrument for centrifugation was MPW-352 centrifuge (MPW MED. Instruments). A centrifugal force of 3000 ± 50 g for 30 min $\pm$ 30 s according to ISO 23714:2014 was used for centrifugation. Fibers were transferred to a pre-weighed dry container and dried for 4 h in 105 °C. The WRV was thereafter calculated according to Eq. 1, where m_1 is the mass of the centrifuged wet fibers and m_2 is dry mass.

$$WRV = \frac{m_1}{m_2} - 1$$

The thermoporometry measurements were based on the protocol developed by Maloney et al. (2023). The measurements were made on a DSC 1 STARe System (Mettler Toledo). The samples were analyzed in sealed aluminum pans with 4–6 mg wet fibers, collected from the centrifuged fibers in the WRV measurements, with addition of 2 mg water to ensure saturation. Samples of pure water were used in order to calculate the specific heat of fusion of water (H_f) later used for the pore volume calculations. The temperature program was: room temperature to -50 °C at 10 °C/min rate, constant temperature at -50 °C

for 10 min, heating to -0.2 °C with a 5 °C/min rate and holding at this temperature for 15 min to ensure melting of all pore water. Thereafter, the temperature was decreased to -50 °C with a rate of 2 °C/min, and finally the sample was heated to 20 °C with 5 °C/min. The pore size distribution (PSD) was analyzed using the freezing exotherm peak from -0.2 down to -20◦C. The temperature depression, ΔT, is related to the pore diameter, D, through the Gibbs–Thomson (GT) equation (Maloney 2015),

$$D = \frac{k}{\Delta T} + 2t_{mono}$$

where k is the GT coefficient (43 nm/°C) and t_{mono} is the monolayer thickness of water 0.28 nm. By using this equation, a pore size distribution between 2–200 nm can be covered.

N_2 sorption

Nitrogen sorption isotherms were measured using a Micromeritics ASAP 2010 instrument. Prior to the measurements about 200 mg fiber samples were placed in sample holders and dried overnight in N_2 at 60 °C. The holders, with free space fillers and isothermal jackets, where then immediately mounted to the instrument to avoid exposure to humidity. The pore size distributions were determined using the BJH (Barrett–Joyner–Halenda) method based on the adsorption isotherms (Barrett et al. 1951), and the specific surface area (SSA) was determined using the BET procedure (Brunauer et al. 1938). The adsorption branch of the isotherm was chosen for the analysis and cylindrical pores where assumed.

Results and discussion

Samples with varied applied stretch before coagulation (draw ratio during spinning) and lignin content were produced to analyze the effect on the pore size distribution. All samples used in this study are summarized in Table 1.

Table 1 Summary of samples used and results from WRV-, Thermoporometry and nitrogen sorption (BJH)-measurements. Pore water (PW) is reported excluding Non-freezing water (NFW) on pore surface. Average/Median standard deviation of, WRV: 0.06/0.03, PW: 0.04/0.05, BET: 0.03/0.008. Samples: 100% coagulate cellulose or cellulose fibers (C), 30% Lignin-70% cellulose fiber (L30), 50% lignin-50% cellulose fiber (L50), delignified L50 fiber (DL L50). Fibers were spun with a draw ratio (DR) of 1 or 2. Samples were analyzed both in Never-dried (ND) and Dried state

Sample	Analysis state	WRV (ml/g)	PW, 2—200 nm (ml/g)	NFW ON PORE SURFACE, 2—200 nm (ml/g)	PORES > 200 nm *(1-PW/WRV)*	Pore volume, BJH (ml/g)
Coagulated cellulose	Never dried	4.19	0.96	0.143	74%	
	Dried	0.93	0.42	0.079	46%	
Cellulose fiber DR 1 (C DR 1)	Never Dried	3.72	0.57	0.090	82%	
	Solvent exchanged	1.04	0.46	0.090	47%	0.27
	Dried	1.05	0.38	0.068	57%	
Cellulose fiber DR 2 (C DR 2)	Never dried	2.47	0.45	0.077	79%	
	Solvent exchange	0.88	0.31	0.066	57%	0.21
	Dried	0.87	0.27	0.055	63%	
30% lignin fiber DR 2 (L30)	Never dried	2.69	0.59	0.091	75%	
	Dried	0.94	0.30	0.062	62%	
50% lignin fiber DR 2 (L50)	Never dried	2.06	0.44	0.089	74%	
	Dried	0.81	0.25	0.054	62%	
Delignified 50% lignin fiber DR 2 (DL L50)	Never dried	2.81	0.54	0.106	77%	
	Solvent exchanged	0.89	0.28	0.060	62%	0.25
Lyocell	Dried	0.74	0.20	0.045	67%	

Pore volume of never-dried and dried cellulose

When fibers swell water is absorbed in the pores, the amorphous domains and in the crystalline amorphous interface (Kulasinski et al. 2015). The results on water retention value (WRV) on the cellulose fibers is presented in Fig. 1. In line with previous studies on cellulosic material, the WRV drastically decreases when going from a never-dried to dried state, indicating severe hornification of the cellulose upon drying. In this work the drying conditions were not varied, however, the pore volume and size distribution can also be tuned by altering the drying conditions (Okubayashi et al. 2005; Salmén and Stevanic 2018).

The measured WRV of the never-dried fibers, for both coagulated without stress and spun fibers, where found to be distinctively higher than reported values for pulp fibers (Mo et al. 2022). From measuring the diameters of never-dried and dried fibers, found in Table S1, the WRV values were considered reliable. The WRV of never-dried cellulose fibers are higher than previously reported WRV for never-dried lyocell fibers (1.85 m/g, Fadavi et al. 2019). This reinforces the trend of lower WRV with increased molecular orientation, since the lyocell fibers likely have higher anisotropy and crystallinity than the fibers prepared within this study (Svenningsson et al. 2019; Cui et al. 2022). The measured WRV for the lyocell fibers are also in line with previously reported values of 0.6 – 0.8 ml/g (Okubayashi et al. 2005; Michels and Kosan 2006). Noteworthy is that lyocell and fibers in this study are prepared using different solvents, and this parameter is also expected to influence the fiber porosity (Zhang et al. 2020). The hornification upon drying, i.e. the difference of WRV for never-dried and dried cellulose, was also found to be less severe for spun fibers (DR 1 and 2) compared to the cellulose coagulated without stress. This indicates that a higher molecular orientation and/or crystallinity aids the preservation of pores during drying.

The WRV includes all pores whereas thermoporometry can only measure pores up to 200 nm in diameter. Thus, by comparing the values of WRV and pore volume obtained from the thermoporometry it is possible to obtain information on fraction of pores larger than 200 nm in diameter. It was found that in the never-dried cellulose approximately 60% of the pores (Table 1) are larger than 200 nm, i.e. large pores. For the dried cellulose samples, the measured value of pore volume in thermoporometry is in the same order of magnitude as the WRV, indicating that it is foremost the large pores that close during drying.

The difference in the amount of pore water measured in thermoporometry indicates that pores within the range of 2 – 200 nm also close during drying. Crawshaw and Cameron also observed decrease in the total pore volume from X-ray measurements on lyocell fibers before and after drying (Crawshaw and Cameron 2000), however they proposed a shift towards fewer but larger pores which is contradictory to what was found in this study. In Figure S1, the decrease in pore water is visualized with the cumulative pore size distribution and it is evident that the pore size distribution shifts toward smaller pores for all dried samples compared to the never dried.

Pore volume in solvent exchanged fibers

Solvent exchange was performed in an attempt of preserving pores going from never-dried to dried state.

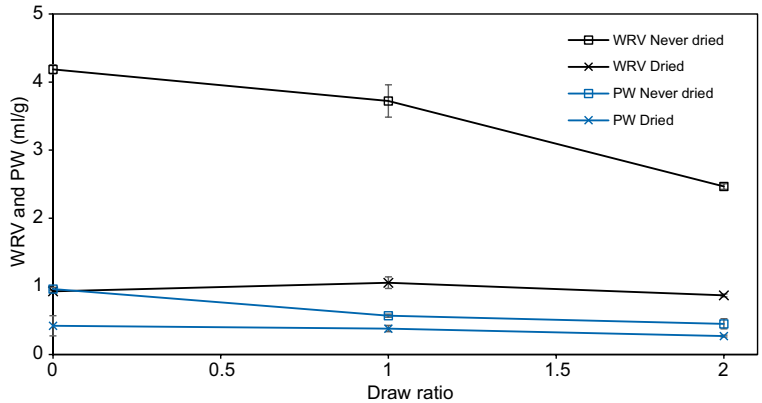

Fig. 1 Water retention values (WRV, black) and Pore water (PW, 2 – 200 nm pores, blue) measured with Thermoporometry for never-dried and dried cellulose. Draw ratio 0 corresponds to cellulose extruded and coagulated without any applied stress (coagulated cellulose). Draw ratio 1 and 2 are spun fibers

The dry solvent-exchanged fibers were used in the nitrogen absorption measurements. In order to further evaluate the effect of solvent exchange on the pore volume, resoaked in water for determination of WRV and thermoporometry. From the WRV values on solvent-exchanged fibers, as well as measurements of fiber diameter, found in Table S1, it was found that the solvent exchange procedure could not completely prevent hornification, i.e. some of the pores in the solvent-exchanged fibers could not regenerated upon rewetting. The WRV of rewetted solvent exchanged fibers is significantly lower than the WRV of the never-dried fibers. The results are in agreement with previous research, as contraction of pulp fibers has been observed upon solvent exchange from water to cyclohexane (Wang et al. 2003).

In fact, the WRV values of solvent exchanged fibers are very similar to that of fibers dried from a water-swollen state. Thus, it seems that the solvent exchange protocol used cannot prevent the largest pores (> 200 nm) from closing. There is however a difference in the pore volume measured with thermoporometry, which is visualized in the pore size distribution, presented in Fig. 2. The solvent-exchanged fibers are found to contain especially more large pores (> 15 nm) compared to the water-dried fibers.

The pore volumes according to the BJH method are lower than the pore volumes measured with thermoporometry. This may partially be explained by the fibers being measured in a water swollen state in the thermoporometry. The pore volume from the BJH method for the two cellulose fibers (DR 1 and 2) follow the same trend as for thermoporometry, with lower pore volume and smaller average pore size (Table S1) for fibers spun with draw ratio 2 compared to 1.

Influence of draw ratio and pore volume

Applying a higher draw ratio in air-gap spinning will, up to a certain level, increase the molecular orientation and crystallinity of the spun fiber (Cai et al. 2010). Moss et al. also found that a higher draw ratio rendered fibers with better oriented voids with smaller diameter (Moss et al. 2002). In this study, a higher draw ratio during spinning resulted in an increased tensile modulus (Table S2), confirming an increased molecular orientation with draw ratio. In compliance with previous studies, an increased molecular orientation also rendered a decreased pore volume of the cellulose fibers. The trend of lowered pore volume with draw ratio is particularly clear for the never-dried cellulose, with a decreasing pore volume with draw ratio for never-dried cellulose both in WRV and pore water (PW) from thermoporometry (squares in Fig. 1). Noteworthy is also that the increased tensile strength with higher draw ratio for the dried fibers (Table S2) may arise from a combination of the increased molecular weight and the lowered pore volume.

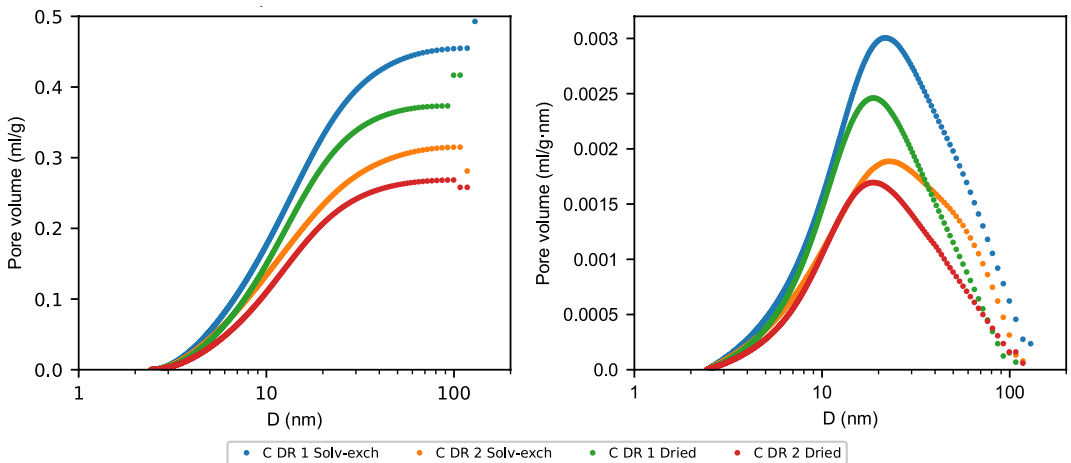

Fig. 2 PSD of solvent exchanged and dried cellulose fibers. Left: cumulative pore size distribution, Right: Pore size distribution based on volume fraction

Noteworthy, the slight difference in pore volume between the dried cellulose samples (x in Fig. 1), becomes more pronounced when extracting the pore size distribution (PSD) from the thermoporometry data, as can be seen in Fig. 3. With increased molecular orientation the pore size distribution is shifted towards smaller pores. The values for the lyocell fibers are consistent with this trend, as they likely have a higher degree of molecular orientation compared to the fibers prepared within this study (Svenningsson et al. 2019; Cui et al. 2022).

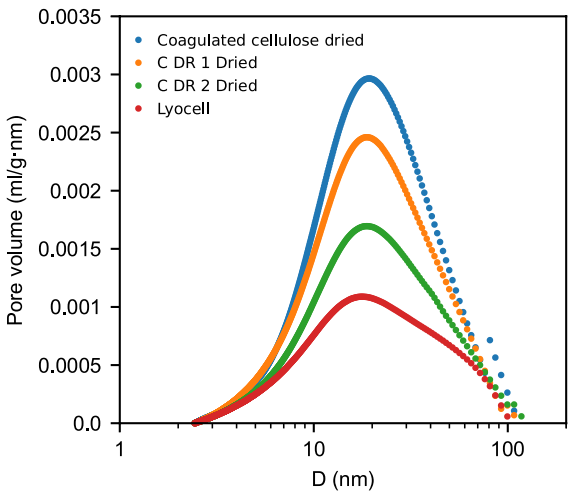

Fig. 3 Pore size distribution based on volume for dried cellulose samples

There is also a substantial decrease in NFW in micropores if comparing fibers spun with draw ratio 1 and 2. This could be due to that the fibers spun with draw ratio 2 are as mentioned likely more crystalline, which limits water absorption. A high draw ratio also induces a higher orientation in the amorphous phase which could further hinder the water accessibility and thus lower the measured NFW in micropores.

Impact of lignin

For fiber containing cellulose and lignin, both never dried and dried, the WRV and PW follow a similar trend, as seen in Fig. 4. When compared to a pure cellulose fiber spun with the same draw ratio, the WRV and PW increases when lignin is added (30%) and is thereafter lowered when the fiber contains even more lignin (50%). It appears that smaller amounts of lignin will interfere with the aggregation of fibrils, act as a spacer, during fiber formation and thus increase fiber swelling (Liu et al. 2023). For larger amounts of lignin, beyond 30%, the lower water sorption of the more hydrophobic lignin probably dominate and swelling is lowered with an incremental increase of lignin content (The WRV of the pure lignin powder was measured to 0.75 ml/g, thus lower than all fibers produced within the study). Noteworthy is also that the surface fiber charge may also impact the WRV, and this may differ between the pure cellulose fibers and the lignin-cellulose fibers (Esteves et al. 2020;

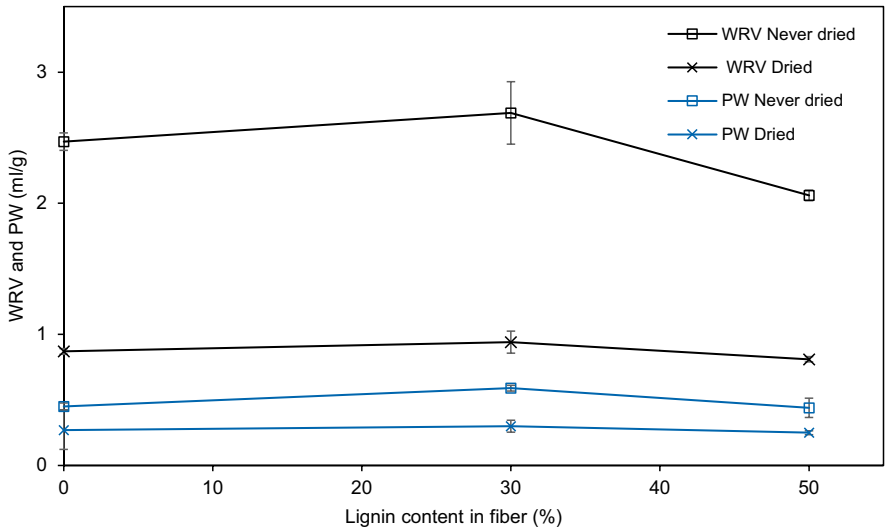

Fig. 4 Water retention values and pore volume from thermoporometry for fibers sun with draw ratio 2 and lignin content of 0 (pure cellulose fiber), 30 and 50%

Maloney et al. 2023), and is thus relevant for future investigations.

The pore size distribution, Fig. 5, reveals that the addition of 30% lignin (L30 DR 2) results in an increased pore volume of foremost small pores compared to the cellulose fiber spun with the same draw ratio (C DR 2).

To obtain more information about where the lignin is located within the fiber and how it affects cellulose aggregation, the pore size distribution of delignified L50 fibers were analyzed as well. The solvent exchange protocol rendered a fiber containing about 8% lignin. Thus, despite lignin being soluble in the acetone–water mixture, some lignin was either enclosed by the cellulose network or strongly interacting with the cellulose and therefore not accessible for delignification.

The pore size distributions of never-dried cellulose fibers, untreated L50 and delignified L50 (DL L50) fibers are presented in Fig. 6. The DL L50 fiber has significantly higher pore volume than the original L50 fiber, and both a widening of the pore size distribution in combination with a slight shift towards larger pores is visible. The change towards larger

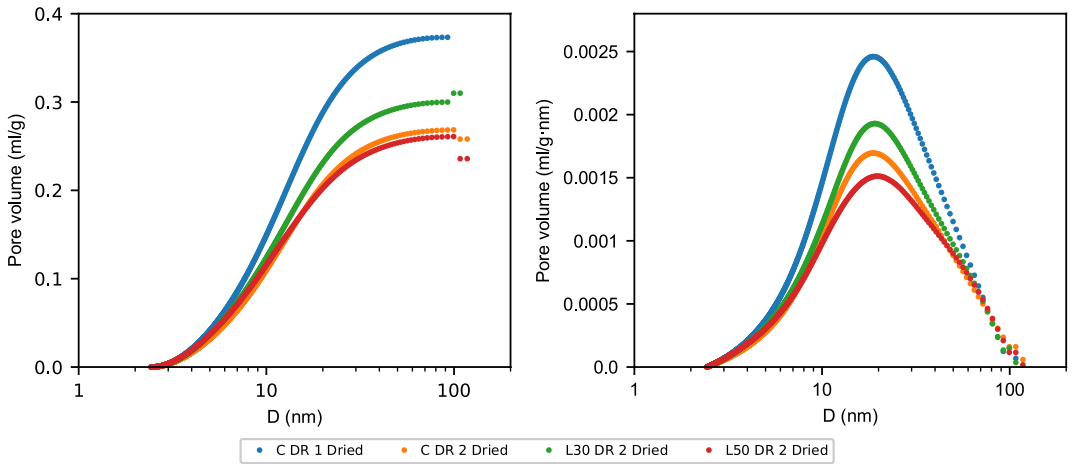

Fig. 5 Pore size distribution for dried cellulose and lignin-cellulose fibers. Left: cumulative pore size distribution, Right: Pore size distribution based on volume fraction

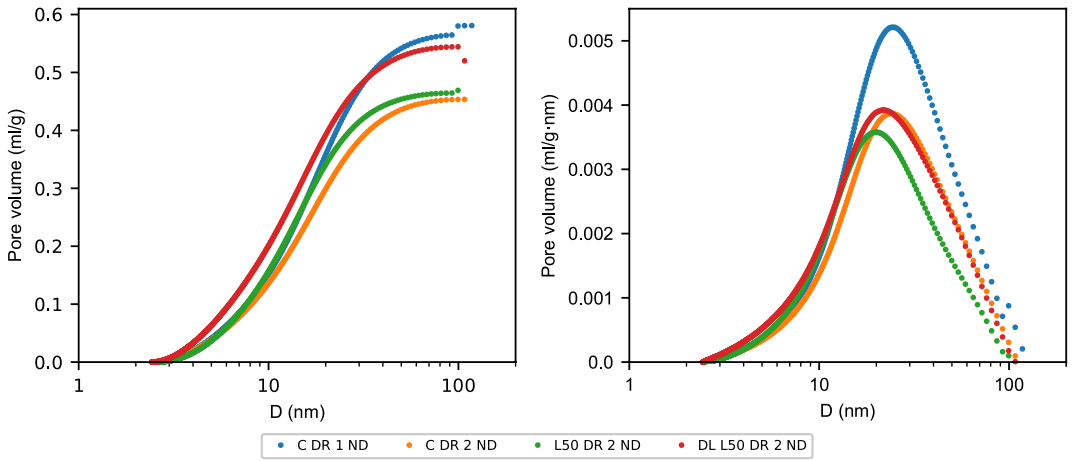

Fig. 6 Pore size distribution for never-dried cellulose, lignin-cellulose fibers and delignified fiber. Left: cumulative pore size distribution, Right: Pore size distribution based on volume fraction

pore volume was hypothesized since we are removing material from the fiber.

Interestingly, however, is the increase in small pores for the DL L50 when comparing to the cellulose fibers. The DL L50 fiber has similar cumulative pore volume as the C DR 1 fiber, but very different PSD with a higher fraction of small pores. This was also confirmed in the N_2 sorption measurements, where C DR 1 had a larger average pore size, based on volume, compared to DL L50, Table S3.

If comparing the PSD of DL L50 with C DR 2 fiber, both spun with draw ratio 2, they mainly differ in the ratio of smaller pores, Fig. 6 right. This indicates that cellulose and lignin mix at a small scale within the fiber, the nm range. The DL L50 also has a higher pore volume than the C DR 2, indicating that lignin disrupts the formation of a dense cellulose network during spinning and creates a more open structure. The result also elucidates the possibility of tuning the porosity of spun fibers by selective dissolution, a common approach for electro-spun fibers (Miranda et al. 2022).

Conclusions

In this study it was found that increased draw ratio lowers the pore volume of the fiber, found in both WRV and thermoporometry. Furthermore, it was found that the pore size distribution shifted towards smaller pores with increased draw ratio. Nitrogen absorption required tedious solvent exchange of the fibers, and the protocol gave a new pore size distribution, not found in either the never dried or dried state. However, nitrogen absorption measurements confirmed the lowered pore volume with increased draw ratio.

When lignin (30%) is added to a cellulose fiber the pore volume increases possibly due to lignin hindering cellulose fibril aggregation. With higher amount of lignin (50%) the pore volume was reported to decrease, although this could be due to the limited water sorption of the hydrophobic lignin. From the pore size distribution, it was also found that the fibers that contained lignin had relatively more small pores compared pure cellulose fibers. Delignified fibers contained an even larger volume of small pores. This indicates that lignin disrupts the cellulose network formation during spinning which results in a more opened microstructure or the fiber.

Thermoporometry enables pore volume measurements of never-dried and dried fibers in a water swollen state, and as a compliment to WRV it also renders the pore size distribution of the sample. This generates further understanding of how differences in the spinning parameters, such as draw ratio, affects the cellulose structure within the fiber.

Acknowledgments This work was funded by the Swedish Research Council for Sustainable Development, Formas [2022-01943].

Author contributions All authors read, reviewed and approved the final manuscript. Specifically, J.B and T.M: Conceptualization, Methodology, J.B, E.J and H.U: Investigation and analysis. J.B: Writing, original draft and figure preparation. T.K: Review and Editing.

Funding Open access funding provided by RISE Research Institutes of Sweden. Swedish Research Council for Sustainable Development, FORMAS [2022–01943].

Data availability No datasets were generated or analysed during the current study.

Declarations

Ethical approval Not applicable.

Competing interests The authors declare no competing interests.

References

Abu-Rous M, Ingolic E, Schuster KC (2006) Visualisation of the fibrillar and pore morphology of cellulosic fibres

applying transmission electron microscopy. Cellulose 13:411–419. https://doi.org/10.1007/s10570-006-9052-5
Abu-Rous M, Varga K, Bechtold T, Schuster KC (2007) A new method to visualize and characterize the pore structure of TENCEL® (lyocell) and other man-made cellulosic fibres using a fluorescent dye molecular probe. J Appl Polym Sci 106:2083–2091. https://doi.org/10.1002/app.26722
Barrett EP, Joyner LG, Halenda PP (1951) The determination of pore volume and area distributions in porous substances. I. Computations from nitrogen isotherms. J Am Chem Soc 73:373–380
Bengtsson A, Bengtsson J, Jedvert K et al (2022) Continuous stabilization and carbonization of a lignin−cellulose precursor to carbon fiber. https://doi.org/10.1021/acsomega.2c01806
Bengtsson A, Bengtsson J, Olsson C et al (2018) Improved yield of carbon fibres from cellulose and kraft lignin. Holzforschung 72:1007–1016. https://doi.org/10.1515/hf-2018-0028
Brunauer S, Emmett PH, Teller E (1938) Adsorption of gases in multimolecular layers. J Am Chem Soc 60:309–319
Cai T, Zhang H, Guo Q et al (2010) Structure and properties of cellulose fibers from ionic liquids. J Appl Polym Sci 115:1047–1053. https://doi.org/10.1002/app.31081
Crawshaw J, Cameron RE (2000) A small angle X-ray scattering study of pore structure in Tencel cellulose fibres and the effects of physical treatments. Polymer (guildf) 41:4691–4698
Cui S, Zhang Y, Liu C et al (2022) The influence of the multilevel structure under high drawing on the preparation of high strength Lyocell fiber. Cellulose 29:751–762. https://doi.org/10.1007/S10570-021-04364-X/TABLES/1
Esteves CSVG, Brännvall E, Östlund S, Sevastyanova O (2020) Evaluating the potential to modify pulp and paper properties through oxygen delignification. ACS Omega 5:13703–13711. https://doi.org/10.1021/acsomega.0c00869
Fadavi F, Abdulkhani A, Hamzeh Y et al (2019) Photodynamic antimicrobial cellulosic material through covalent linkage of protoporphyrin IX onto Lyocell fibers. J Wood Chem Technol 39:57–74. https://doi.org/10.1080/02773813.2018.1500605
Fang W, Fan R, Aranko AS et al (2023) Upcycling of keratin wastes in sustainable textile fiber applications. ACS Sustain Chem Eng 11:14807–14815. https://doi.org/10.1021/ACSSUSCHEMENG.3C04987/ASSET/IMAGES/LARGE/SC3C04987_0006.JPEG
Gubitosi M, Asaadi S, Sixta H, Olsson U (2021) The colloidal structure of a cellulose fiber. Cellulose 28:2779–2789. https://doi.org/10.1007/S10570-021-03711-2/FIGURES/4
Hedlund A, Köhnke T, Hagman J et al (2019) Microstructures of cellulose coagulated in water and alcohols from 1-ethyl-3-methylimidazolium acetate: contrasting coagulation mechanisms. Cellulose 26:1545–1563. https://doi.org/10.1007/s10570-018-2168-6
Hermansson F, Janssen M, Svanström M (2019) Prospective study of lignin-based and recycled carbon fibers in composites through meta-analysis of life cycle assessments. J Clean Prod 223:946–956. https://doi.org/10.1016/j.jclepro.2019.03.022
Hribernik S, Stana Kleinschek K, Rihm R et al (2016) Tuning of cellulose fibres' structure and surface topography: Influence of swelling and various drying procedures. Carbohydr Polym 148:227–235. https://doi.org/10.1016/j.carbpol.2016.04.053
Kammiovirta K, Jääskeläinen AS, Kuutti L et al (2016) Keratin-reinforced cellulose filaments from ionic liquid solutions. RSC Adv 6:88797–88806. https://doi.org/10.1039/C6RA20204G
Köhnke T, Östlund Å, Brelid H (2011) Adsorption of arabinoxylan on cellulosic surfaces: influence of degree of substitution and substitution pattern on adsorption characteristics. Biomacromol 12:2633–2641. https://doi.org/10.1021/bm200437m
Koistinen A, Phiri J, Kesari KK et al (2023) Effect of pulp prehydrolysis conditions on dissolution and regenerated cellulose pore structure. Cellulose 30:2827–2840. https://doi.org/10.1007/s10570-023-05050-w
Kongdee A, Bechtold T, Burtscher E, Scheinecker M (2004) The influence of wet/dry treatment on pore structure-the correlation of pore parameters, water retention and moisture regain values. Carbohydr Polym 57:39–44. https://doi.org/10.1016/j.carbpol.2004.03.025
Kulasinski K, Guyer R, Derome D, Carmeliet J (2015) Water adsorption in wood microfibril-hemicellulose system: role of the crystalline-amorphous interface. Biomacromol 16:2972–2978. https://doi.org/10.1021/acs.biomac.5b00878
Larsson PT, Svensson A, Wågberg L (2013) A new, robust method for measuring average fibre wall pore sizes in cellulose I rich plant fibre walls. Cellulose 20:623–631. https://doi.org/10.1007/s10570-012-9850-x
Liu J, Bengtsson J, Yu S et al (2023) Variation in the hierarchical structure of lignin-blended cellulose precursor fibers. Int J Biol Macromol 225:1555–1561. https://doi.org/10.1016/j.ijbiomac.2022.11.211
Luukko K, Maloney TC (1999) Swelling of mechanical pulp fines. Cellulose 6:123–135
Ma Y, Asaadi S, Johansson LS et al (2015) High-strength composite fibers from cellulose-lignin blends regenerated from ionic liquid solution. Chemsuschem 8:4030–4039. https://doi.org/10.1002/cssc.201501094
Maloney T, Phiri J, Zitting A et al (2023) Deaggregation of cellulose macrofibrils and its effect on bound water. Carbohydr Polym 319:121166. https://doi.org/10.1016/j.carbpol.2023.121166
Maloney TC (2015) Thermoporosimetry of hard (silica) and soft (cellulosic) materials by isothermal step melting. J Therm Anal Calorim 121:7–17. https://doi.org/10.1007/s10973-015-4592-2
Michels C, Kosan B (2006) Beitrag zur Struktur von Lyocellfasern, ersponnen aus Aminoxidhydraten bzw. Ionischen Flussigkeiten. Lenzinger Berichte 86:144–153
Michud A, Hummel M, Sixta H (2016) Influence of process parameters on the structure formation of man-made cellulosic fibers from ionic liquid solution. J ApplPolym Sci 133. https://doi.org/10.1002/app.43718
Miranda CS, Silva AFG, Pereira-Lima SMMA et al (2022) Tunable spun fiber constructs in biomedicine: influence of processing parameters in the fibers' architecture. Pharmaceutics 14(1):164. https://doi.org/10.3390/pharmaceutics14010164
Mo W, Chen K, Yang X et al (2022) Elucidating the hornification mechanism of cellulosic fibers during the process of

thermal drying. Carbohydr Polym 289:119434. https://doi.org/10.1016/J.CARBPOL.2022.119434

Moss CE, Butler MF, Müller M, Cameron RE (2002) Microfocus small-angle X-ray scattering investigation of the skin–core microstructure of lyocell cellulose fibers. J Appl Polym Sci 83(13):2799–2816. https://doi.org/10.1002/app.10256

Okubayashi S, Griesser UJ, Bechtold T (2005) Water accessibilities of man-made cellulosic fibers - effects of fiber characteristics. Cellulose 12:403–410. https://doi.org/10.1007/s10570-005-2179-y

Östlund Å, Idström A, Olsson C et al (2013) Modification of crystallinity and pore size distribution in coagulated cellulose films. Cellulose 20:1657–1667. https://doi.org/10.1007/s10570-013-9982-7

Ota A, Beyer R, Hageroth U et al (2021) Chitin/cellulose blend fibers prepared by wet and dry-wet spinning. Polym Adv Technol 32:335–342. https://doi.org/10.1002/PAT.5089

Protz R, Lehmann A, Bohrisch J et al (2021) Solubility and spinnability of cellulose-lignin blends in specific ionic liquids. Carbohydr Polym Technol Appl 2:100041. https://doi.org/10.1016/j.carpta.2021.100041

Salmén L, Stevanic JS (2018) Effect of drying conditions on cellulose microfibril aggregation and "hornification." Cellulose 25:6333–6344. https://doi.org/10.1007/S10570-018-2039-1/FIGURES/10

Sharma A, Sen D, Thakre S, Kumaraswamy G (2019) Characterizing microvoids in regenerated cellulose fibers obtained from viscose and lyocell processes. Macromolecules 52:3987–3994. https://doi.org/10.1021/ACS.MACROMOL.9B00487/SUPPL_FILE/MA9B00487_SI_001.PDF

Shen L, Worrell E, Patel MK (2012) Comparing life cycle energy and GHG emissions of bio-based PET, recycled PET, PLA, and man-made cellulosics. Biofuels, Bioprod Biorefin 6:625–639. https://doi.org/10.1002/bbb.1368

Svenningsson L, Sparrman T, Bialik E et al (2019) Molecular orientation distribution of regenerated cellulose fibers investigated with rotor synchronized solid state NMR spectroscopy. Cellulose 26:4681–4692. https://doi.org/10.1007/S10570-019-02430-Z/TABLES/2

Wang X, Maloney T, Paulapuro H (2003) Internal fibrillation in never-dried and once-dried chemical pulps. Appita J 56:455–459

Zhang J, Tominaga K, Yamagishi N, Gotoh Y (2020) Comparison of regenerated cellulose fibers spun from ionic liquid solutions with Lyocell fiber. J Fiber Sci Technol 76:257–266. https://doi.org/10.2115/FIBERST.2020-0029

Zhang YQ, Lykaki M, Alrajoula MT et al (2021) Microplastics from textile origin – emission and reduction measures. Green Chem 23:5247–5271. https://doi.org/10.1039/D1GC01589C